Int. J. Electrochem. Sci., 16**(2021)** Article Number: 211112, doi: 10.20964/2021.11.17

International Journal of
ELECTROCHEMICAL
SCIENCE
www.electrochemsci.org

Synthesis of Nanocomposites Based on Gold and Nickel as Sensitive Electrochemical Sensor for Determination of Salmonella Typhimurium in Food Industry

Huixing Li[1,2,*], *Haiyan Yu*[1,2] *and Xiancai Zeng*[1,2]

[1] Henan Key Laboratory of Industrial Microbial Resources and FermentationTechnology, Nanyang Institute of Technology, Nanyang, Henan 473004, China
[2] School of Biological and Chemical Engineering, Nanyang Institute of Technology, Nanyang, Henan 473004, China
[*]E-mail:HuixingLi@protonmail.com

Received: 18 July 2021/ *Accepted:* 25 August 2021 / *Published:* 10 October 2021

In this work, an electrochemical sensor based on gold and Nickel nanoparticles decorated on nanocomposites of c-CNTs and PEDOT modified GCE was developed to determine Salmonella as a poisoning microorganism in food samples. The electrodeposition method was applied for the synthesis of bimetallic Au-Ni nanoparticles on a nanocomposite of c-CNTs and PEDOT modified GCE (Au-Ni NPs/c-CNTs-PEDOT/GCE), and the anti-Salmonella Typhimurium antibodies were immobilized on modified GCE (Ab/Au-Ni NPs/c-CNTs-PEDOT/GCE). The structural analyses using SEM, XRD and EDS showed that the high densities of bimetallic nanoparticles were distributed on rod-like and porous structures of c-CNTs-PEDOT. An electrochemical study using CV and DPV techniques showed Ab/Au-Ni NPs/c-CNTs-PEDOT/GCE was a sensitive, stable and selective Salmonella sensor. The linear range, limit of detection and sensitivity were obtained 1-120 µM, 0.64 nM and 4.6789µA/µM, respectively. Comparison of the sensing properties of this study with the other reported Salmonella sensors indicated the broad linear range was obtained for Ab/Au-Ni NPs/c-CNTs-PEDOT/GCE that was attributed to the capture of Salmonella on Au-Ni NPs-labeled antibodies which are placed on the porous network c-CNTs-PEDOT/GCE. The prepared sensor was examined for determination of Salmonella in a real sample of egg and the results illustrated the acceptable values of recovery (91 to 98.5%) and RSD (2.84 to 3.71%) which is attributed to validation and precision of this method for analyses of food samples.

Keywords: Salmonella; Differential pulse voltammetry; Bimetallic Au-Ni nanoparticles; Carboxylated CNTs; Electrodeposition

1. INTRODUCTION

Salmonella as important intracellular pathogens of Enterobacteriaceae is a Gram-negative bacteria that cause foodborne illness [1, 2]. Salmonella is a chemotroph microorganism which means it

can obtain its energy from the aerobic oxidation or reduction reactions of organic compounds. This is also a facultative anaerobe that is capable to generate adenosine triphosphate with oxygen in the presence and absence of oxygen through the use of other electron acceptors or fermentation [3, 4]. Salmonella can happen in raw poultry, chicken, pork, beef, eggs and milk which are not cooked enough, and sometimes are found in nuts, sprouts and unwashed fruit and vegetables [5]. Therefore, Salmonella can be considered as a poisoning microorganism in the food industry.

Salmonella may also be found in the feces of some pets such as turtles, lizards, other reptiles and chicks especially those with diarrhea, and people who have these animals who can become infected [6]. Infected People can also spread the bacteria to other people, objects, and surfaces.

Salmonella species as intracellular pathogens usually invade the gastrointestinal tract and cause food-borne infection and salmonellosis, paratyphoid fever, typhoid fever, hypovolemic shock and septic shock which require intensive care including antibiotics. Children with immune system problems are at higher risk for more severe illness [7]. Thus, many studies have been performed using molecular methods, high-performance liquid chromatography, aptamer-based fluorometry, colorimetry and electrochemistry to development the Salmonella detection techniques [8-11]. Among these methods, electrochemical detection technique as low cost and fast sensing system can be developed by modification the electrode surface with nanomaterials and composites. Furthermore, the immobilization of the biomaterials can increase the selectivity and sensitivity of sensors [12-14].

Therefore, this study was performed for fabrication of nanocomposites based on gold and Nickel as sensitive electrochemical sensor for determination of Salmonella as poisoning microorganism in food samples.

2. MATERIALS and METHOD

2.1. Synthesis of Ab/Au-Ni NPs/c-CNTs-PEDOT/GCE

The GCE surface was cleaned through the polishing using alumina slurry (0.3 and 0.05 µm, ≥99%, Sigma-Aldrich) on micro cloth pad for 15 minutes, and ultrasonically washing with deionized water and ethanol for 10 minutes, respectively. For functionalization of CNTs walls with negatively charged carboxyl groups (CNTs-COOH) [15], 100 mg of CNTs (>95%, Beijing Dingsheng Brothers Technology Co., Ltd., China) was ultrasonically added in a mixture of 15ml of H_2SO_4 (95%, Merck Millipore, Germany) and 5ml of HNO_3 (65% Merck Millipore, Germany) for two hours. Next, carboxylated CNTs (c-CNTs) was ultrasonically washed by DI water, and then dispersed in a mixture of ethanol and deionized water in equal volume ratio and dried in an oven at 60°C for 1 hour. After then, 4mg of c-CNTs was homogeneously dispersed in 4ml of poly(3,4-ethylenedioxythiophene) (PEDOT, 97%, Sigma-Aldrich) and to achieve a uniform mixture as the electrolyte solution. All electrochemical studies and electrodepositions were conducted on an electrochemical work station (CHI 660E, Shanghai Chenhua Instrument Co. Ltd., China) using a three-electrode system that it was contained Pt foil as counter, Ag/AgCl (3M KCl) as reference and GCE or modified GCE as the working electrode. Subsequently, the electrodeposition of c-CNTs-PEDOT nanocomposite on clean

GCE (c-CNTs-PEDOT/GCE) was carried out through cyclic voltammetry (CV) at a potential range from −1.3 V to 1.2 V at a scan rate of 100 mV/s for 7 minutes [16].

For electrodeposition of bimetallic alloy of Au-Ni nanoparticles on c-CNTs-PEDOT/GCE (Au-Ni NPs/c-CNTs-PEDOT/GCE) [17, 18], the electrolyte was prepared from mixture of 0.03 M AuCl (99%, Sigma-Aldrich) and 0.13 M $NiSO_4$ (≥99%, Sigma-Aldrich) solutions in equal volume ratio. The electrodeposition was performed through CV at a potential range from −0.3 V to −1.6 V at a scan rate of 20mV/s for 15 minutes.

For immobilization of anti-Salmonella typhimurium antibodies on Au-Ni NPs/c-CNTs-PEDOT/GCE, the electrode was immersed in a 1 ml mixture solution of 0.1 M 4-morpholineethanesulfonic acid (≥99%, Sigma-Aldrich) and 0.5 M NaCl (99%, Merck Millipore, Germany) in an equal volume ratio for 20 minutes. Next, 10 mg of 1-ethyl-3-(3-dimethylaminopropyl) carbodiimide (99%, Sigma-Aldrich) and 20 mg of *N*-hydroxysuccinimide (98%, Sigma-Aldrich) was added to the mixture solution under magnetic stirring, and then the electrode was immersed in this mixture for 20 minutes. After then, the electrode immersed in 1 mg/mL anti-Salmonella typhimurium antibody (Sigma-Aldrich) solution for 120 minutes. Finally, the anti-Salmonella antibodies conjugated modified GCE (Ab/Au-Ni NPs/c-CNTs-PEDOT/GCE) was rinsed with 0.1 M phosphate buffer solution (PBS) pH 6.0 and stored in the refrigerator at 4°C for electrochemical studies.

2.2. Preparation the real sample

The real samples of regular eggs were purchased from the local market. The liquid of egg samples were homogenized with a high-speed blender. 1 ml of 2 mM Salmonella typhimurium (S. typhi, >95%, Sigma-Aldrich) has added to 10ml of egg samples. Next, 10 mL of 0.1 M PBS was added the samples under the magnetic string that resulted in the 0.1 µM S. typhi. Afterward, the prepared sample was stored in the refrigerator at 4 °C for electrochemical analysis.

2.3. Analyses

Cyclic voltammetry (CV) CV and differential pulse voltammetry (DPV) studies were performed at 20mV/s scanning rate in 0.1M PBS pH 6.0 as an electrolyte which prepared from 0.1M H_3PO_4 (99%, Sigma-Aldrich) and 0.1M NaH_2PO_4 (99%, Sigma-Aldrich). The microstructure of the nanostructured films was analyzed using a scanning electron microscopy (SEM, JEOL, JSM 6300F apparatus). The crystal structure was studied using X-ray diffraction (XRD, X'Pert Pro Super, Philips Co., the Netherlands). The chemical composition of the material was studied using energy-dispersive X-ray spectroscopy (EDS, JEOL, 7600F, Japan)

3. RESULT AND DISCUSSION

2.1. Structural study

FESEM images of c-CNTs dispersion in ethanol in Figure 1a shows the highly porous 3D network of CNTs with a diameter of ~45 nm. SEM image of Au-Ni NPs/c-CNTs-PEDOT/GCE in Figure 1b shows that the nanoparticles were distributed on rod-like of c-CNTs-PEDOT. As seen, Au-Ni NPs are randomly decorated along sidewalls c-CNTs-PEDOT. There is no agglomeration of electrodeposited Au-Ni NPs that can be associated with the high nucleation site and large aspect ratio of c-CNTs-PEDOT [19, 20]. The average diameter of Au-Ni NPs is ~25 nm.

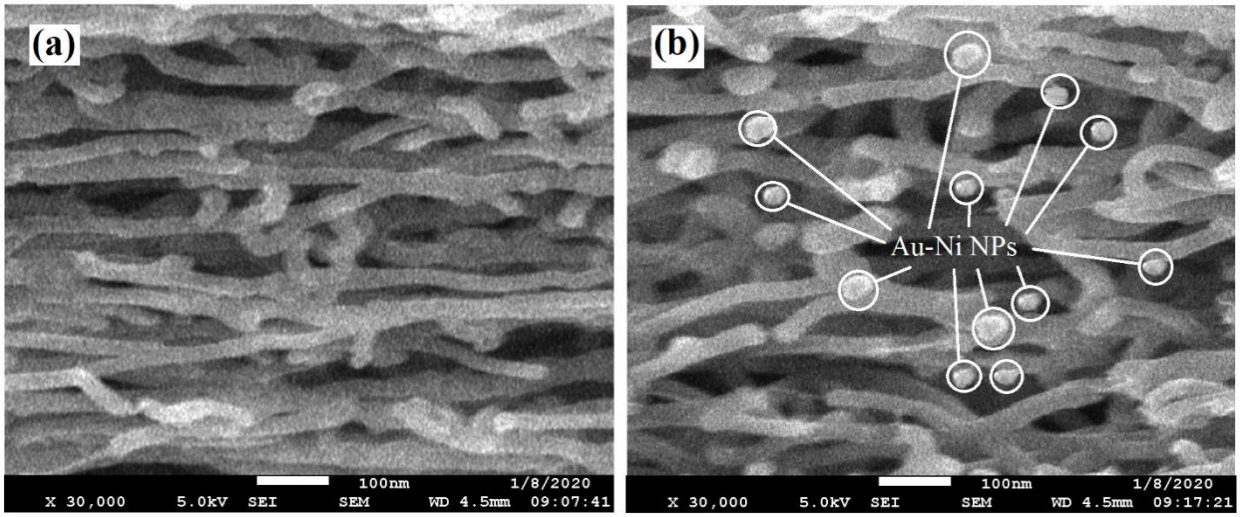

Figure 1. SEM image of (a) c-CNTs dispersion in ethanol, (b) Au-Ni NPs/c-CNTs-PEDOT/GCE.

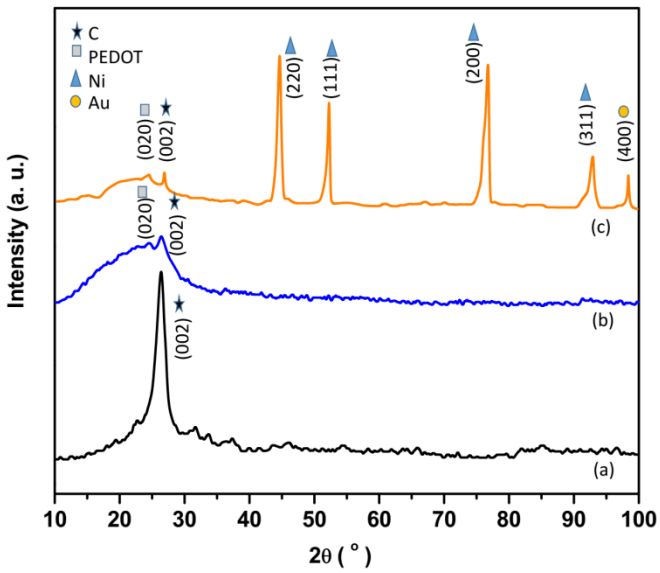

Figure 2. XRD pattern of (a) c-CNTs, (b) c-CNTs-PEDOT and (c) Au-Ni NPs/c-CNTs-PEDOT

XRD pattern of c-CNTs, c-CNTs-PEDOT and Au-Ni NPs/c-CNTs-PEDOT are shown in Figure 2. The XRD patterns of c-CNTs show the single sharp peak at 26.33° which corresponding to the (002) graphitic plane [21]. As observed from Fig. 2b, XRD patterns of c-CNTs-PEDOT show the broad peak at 24.58° that it related to (020) planes of the orthorhombic unit cell of the PEDOT crystal [22]. In addition, the intensity of peak (002) of c-CNTs was decreased because of the amorphous nature of PEDOT which is similar to other reports [23]. The XRD patterns of Au-Ni NPs/c-CNTs-PEDOT/GCE shows the additional peaks at 44.80°, 52.31°, 76.50° and 92.56° which related to (220), (111), (200), and (311) fcc crystal planes of Ni (*JCPDS card No.* 04-0850), and peak at 98.42° which corresponding to (400) fcc plane of Au (JCPDS card No. 04-0784).

Figure 3 exhibits EDS spectra of Au-Ni NPs/c-CNTs-PEDOT which illustrates the presence of Au and Ni metals in the prepared heterostructure. Moreover, the presence of elements of C, O and S is attributed to the chemical composition of c-CNTs-PEDOT. The results of SEM. XRD and EDS are indicated to successful electrodeposition of c-CNTs-PEDOT on GCE and Au-Ni NPs on c-CNTs-PEDOT.

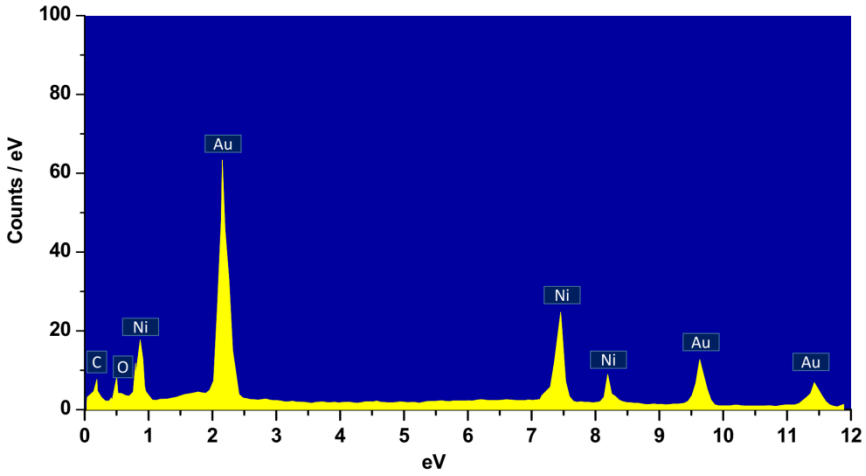

Figure 3. EDS spectra of Au-Ni NPs/c-CNTs-PEDOT.

2.2. Electrochemical study

Figure 4 shows the electrochemical behavior of GCE, PEDOT/GCE, c-CNTs/GCE, c-CNTs-PEDOT/GCE, Au-Ni NPs/c-CNTs-PEDOT/GCE and Ab/Au-Ni NPs/c-CNTs-PEDOT/GCE in presence of 0.5 µM S. typhi solution in 0.1 M PBS pH 6.0 at a scanning rate of 20 mV/s. As seen, one reduction peak at -0.33, -0.2, -0.14, -0.13, -0.19 and -0.2 V is observed for CV curves of GCE, PEDOT/GCE, c-CNTs/GCE, c-CNTs-PEDOT/GCE and Au-Ni NPs/c-CNTs-PEDOT/GCE, respectively, and no oxidation peak is found for all electrodes which indicated that the electrochemical reaction of S. typhi on the all electrodes surfaces is an irreversible process . The poor reduction peak is observed for GCE (-0.28 µA) which is slightly enhanced by modification of GCE surface with PEDOT (-0.68 µA) which can be related to the improvement of the conductivity PEDOT/GCE [24]. The

obvious improvements of reduction peak current are observed to c-CNTs/GCE (-1.27 μA) due to the extremely high surface-to-volume ratio, geometry, high surface adsorptive ability, and hollow structure of c-CNTs [25-27]. As observed, c-CNTs-PEDOT/GCE shows that the reduction peak current (-2.31 μA) is approximately two and three times more than c-CNTs/GCE and PEDOT/GCE which is related to the synergistic effect between the PEDOT and c-CNTs components of hybrid film and formation of 3D porous network in agreement with SEM results [28]. Au-Ni NPs/c-CNTs-PEDOT/GCE shows the increase of electrocatalytic current (-3.37 μA) due to the 3D porous network of c-CNTs-PEDOT/GCE that provided a large platform for electrodepositing bimetallic nanoparticles and the small spherical nanoparticles bimetallic which generates a porous structure and larger specific surface area [29-31]. Furthermore, very small dimensions of electrodeposited bimetallic nanoparticles on porous network and defect sites of c-CNTs-PEDOT composite enhance electrical conductivity and facilitate diffusion rates and fast electron transfer kinetics defect sites [32]. The highest electrocatalytic current (-4.80 μA) are observed for Ab/Au-Ni NPs/c-CNTs-PEDOT/GCE because of Salmonella bound to both the capture and Au-Ni NPs-labeled antibodies which are placed on the c-CNTs-PEDOT/GCE. The electrodeposited Au-Ni NPs on the 3D porous network of c-CNTs-PEDOT create a platform for the conjugation of antibody molecules [33]. Thus, the following electrochemical studies were performed on Ab/Au-Ni NPs/c-CNTs-PEDOT/GCE.

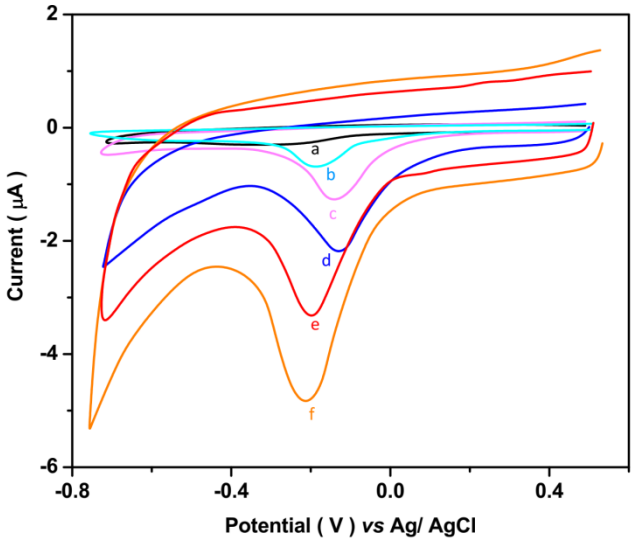

Figure 4. CV curves of GCE, PEDOT/GCE, c-CNTs/GCE, c-CNTs-PEDOT/GCE, Au-Ni NPs/c-CNTs-PEDOT/GCE and Ab/Au-Ni NPs/c-CNTs-PEDOT/GCE in presence of 0.5 μM S. typhi solution in 0.1 M PBS pH 6.0 at scanning rate of 20mV/s.

The stability of electrochemical behavior of Ab/Au-Ni NPs/c-CNTs-PEDOT/GCE was investigated through the record of successive CVs in presence of 0.5 μM S. typhi solution in 0.1 M PBS pH 6.0 at scanning rate of 20 mV/s. Figure 5 depicts first, second and 100th recorded CVs of the electrode which demonstrated the change of reduction peak of S. typhi at -0.2 V between the first and

second CVs is inconsiderable (>2%).However, the decrease in reduction peak current after successive 100 sweeps is 6% for Ab/Au-Ni NPs/c-CNTs-PEDOT/GCE, evidence to the excellent stability of Ab/Au-Ni NPs/c-CNTs-PEDOT/GCE because of anti-fouling properties of PEDOT and strong π-π interactions between conjugated PEDOT, c-CNTs and Au-Ni NPs through construction of chemical Au–S, Au-C and Ni–C bonds[34-36]. Moreover, direct covalent bond between Au and a thiolated antibody promote the stability of the sensor [33].

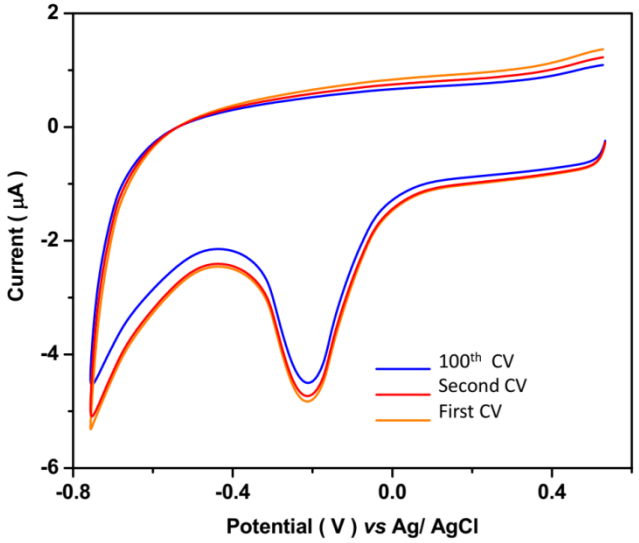

Figure 5. First, second and 100th recorded CVs of Ab/Au-Ni NPs/c-CNTs-PEDOT/GCE in presence of 0.5 μM S. typhi solution in 0.1M PBS pH 6.0 at scanning rate of 20mV/s.

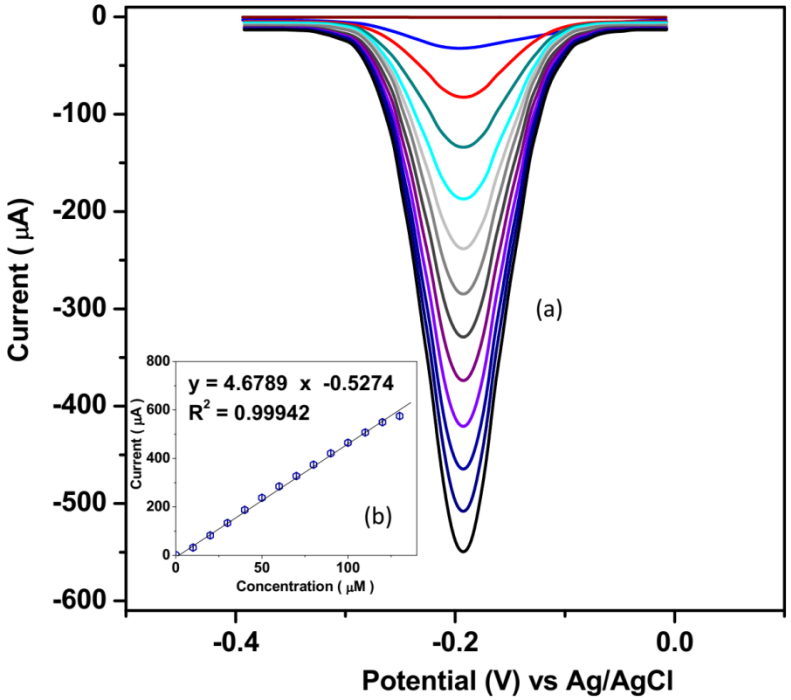

Figure 6. (a) The DPV curves and (b) obtained calibration plot of Ab/Au-Ni NPs/c-CNTs-PEDOT/GCE under successive addition of S. typhi solution in 0.1M PBS pH 6.0 at 20mv/s scanning rate.

The DPV technique was applied to evaluate the sensing properties of Ab/Au-Ni NPs/c-CNTs-PEDOT/GCE for detection of S. typhi. Figure 6 exhibits the DPV curves and obtained calibration plot of the proposed modified electrode under successive addition of S. typhi solution in 0.1M PBS pH 6.0 at a scanning rate of 20mv/s. It can be observed that peak currents are increased linearly with an injection of S. typhi solution. The linear range, limit of detection (LOD) and sensitivity of Ab/Au-Ni NPs/c-CNTs-PEDOT/GCE are obtained 1-120 µM, 0.64 nM and 4.6789 µA/µM, respectively, which compared by the other reported Salmonella sensors (Table 1), indicating the broad linear range is obtained for Ab/Au-Ni NPs/c-CNTs-PEDOT/GCE that it is attributed to capture of Salmonella on Au-Ni NPs-labeled antibodies which are placed on the porous network c-CNTs-PEDOT/GCE. Moreover, the use of Ni and PEDOT to enhance the stability and linear range, and reduce the cost of modified electrode GCE toward the modified Au and Pt-based electrodes in [10, 37-40] can be the advantage of this study.

Table 1. Comparison of the sensing properties of Ab/Au-Ni NPs/c-CNTs-PEDOT/GCE with the other reported Salmonella sensors.

Electrode	**Technique**	**Linear Range (µM)**	**limit of detection (nM)**	**ref**
Ab/Au-Ni NPs/c-CNTs-PEDOT/GCE	DPV	1-120	0.64	This work
Methylene blue -labeled DNA probe/Au	DPV	0.06-0.3	60	[37]
ssDNA/Ru-Fe complex /GCE	square wave voltammetry	0.4–0.8	400	[41]
ssDNA/6-mercapto-1-hexanol/ Au	square wave voltammetry	10^{-6}–0.01	5×10^{-4}	[42]
DNAzyme probe self-assembled Au NPs	UV–vis	0.005–0.05	0.44	[38]
ssDNA/Au	Alternating current voltammetry	0.025–2.4	10^{-5}	[39]
Pyrroquinolinequinone/glucose dehydrogenase -DNA/ Carbon paste electrode	Amperometry	0.05–10	500	[43]
ssDNA/Pt/Au	Electrochemical impedance spectroscopy	0.001–0.5	1	[40]
ssDNA/ Salmonella chip	Surface plasmon resonance	0.005–1	0.5	[44]

The further electrochemical study was conducted on Ab/Au-Ni NPs/c-CNTs-PEDOT/GCE for investigation of interference effect on S. typhi determination. Table 2 reveals the results of electrocatalytic peak currents of DPV of Ab/Au-Ni NPs/c-CNTs-PEDOT/GCE in 0.1M PBS pH 6.0 at

20mv/s scanning rate in successive additions of 1 µM S. typhi solution and 10 µM of E. coli, S. enteritis, P. aeruginosa, L. monocytogenes and L. innocua as foodborne pathogens [45]. As observed, the modified electrode indicates an obvious electrocatalytic signal to the addition of S. typhi solution and there are no significant electrocatalytic signals for the additions of other species which represented the selective response of Ab/Au-Ni NPs/c-CNTs-PEDOT/GCE to the determination of S. typhi. In addition, specific antigen and antibody binding is important to selective detection of Salmonella [46].

Table 2. Resulted electrocatalytic peak currents of DPV of Ab/Au-Ni NPs/c-CNTs-PEDOT/GCE in 0.1M PBS pH 6.0 at 20mv/s scanning rate in successive additions of 1 µM S. typhi solution and 10 µM of various foodborne pathogens.

Specie	**Concentration (µM)**	**electrocatalytic peak current (µA)**	**RSD* (%)**
S. typhi	1	4.681	±0.075
E. coli	10	0.101	±0.013
S. enteritis	10	0.087	±0.009
P. aeruginosa	10	0.093	±0.009
L. monocytogenes	10	0.100	±0.017
L. innocua	10	0.077	±0.008

* relative standard deviation

Applicability of the Ab/Au-Ni NPs/c-CNTs-PEDOT/GCE was examined for determination of S. typhi in 0.1M PBS pH 6.0 containing prepared real sample of egg through DPV technique at 20mv/s scanning rate. Figure 7 shows the DPV response and obtained calibration plot of the proposed sensor to successive additions of 1 µM S. typhi solutions. As observed, the content of S. typhi in electrochemical cell of the prepared specimens of the egg in 0.1M PBS is 0.097 µM that it is in agreement with the initial added value of S. typhi in blended eggs. Table 2 also presents the acceptable values of recovery (91 to 98.5%) and RSD (2.84 to 3.71%) which are attributed to the validation and precision of this method for analyses of food samples.

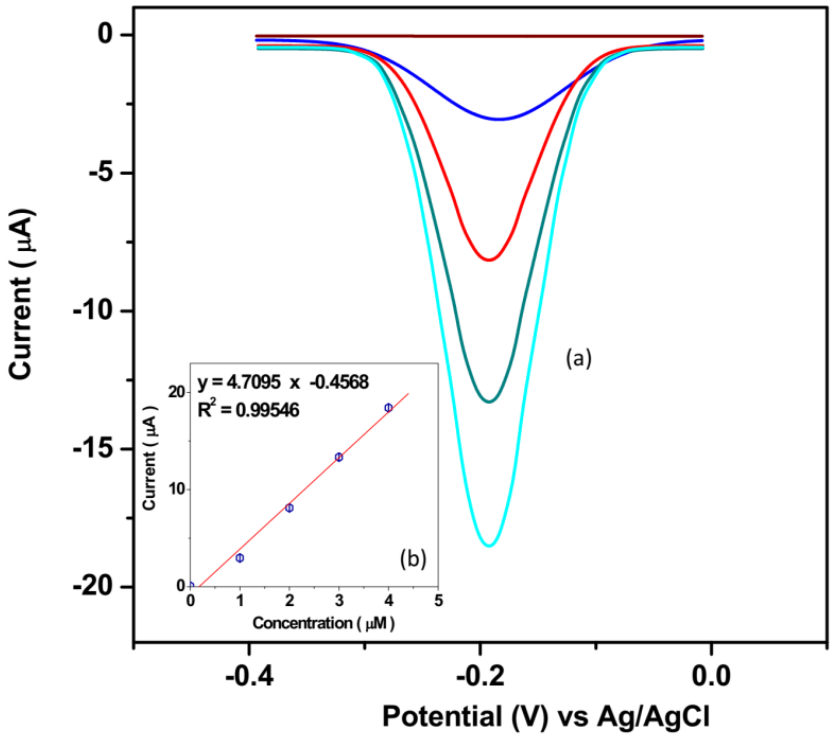

Figure 7. (a) DPV response and (b) obtained calibration plot of Ab/Au-Ni NPs/c-CNTs-PEDOT/GCE for detection of S. typhiin 0.1 M PBS pH 6.0 containing prepared real sample of eggat scanning rate of 20 mv/s.

Table 3. Analytical Result of practical determination of S. typhiprepared real sample of egg(n = 4)

Added(μM)	Fund(μM)	Recovery(%)	RSD(%)
1.00	0.91	91.00	2.84
2.00	1.87	93.50	3.05
3.00	2.92	97.33	3.11
4.00	3.94	98.50	3.71

4. CONCLUSION

This study was performed for fabrication of Ab/Au-Ni NPs/c-CNTs-PEDOT/GCE as sensitive electrochemical sensor for detection of Salmonella as poisoning microorganism in food samples. For the synthesis of the sensor, nanocomposite of c-CNTs and PEDOT was electrodeposited on GCE, then, a bimetallic alloy of Au-Ni nanoparticles was electrodeposited on c-CNTs-PEDOT/GCE. After then, the anti-Salmonella typhimurium antibodies were immobilized on modified GCE. The structural analyses showed that the high density of bimetallic nanoparticles was distributed on the rod-like and

porous structure of c-CNTs-PEDOT. Electrochemical study showed Ab/Au-Ni NPs/c-CNTs-PEDOT/GCE was sensitive, stable and selective Salmonella sensor. The linear range, LOD and sensitivity were obtained 1-120 µM, 0.64 nM and 4.6789 µA/µM, respectively. Comparison of the sensing properties of this study with the other reported Salmonella sensors indicated the broad linear range was obtained for Ab/Au-Ni NPs/c-CNTs-PEDOT/GCE that it was attributed to capture of Salmonella on Au-Ni NPs-labeled antibodies which are placed on the porous network c-CNTs-PEDOT/GCE. Applicability of the prepared sensor was examined for determination of S. typhi in the prepared real sample of egg and results illustrated the acceptable values of recovery and RSD which are attributed to the validation and precision of this method for analyses of food samples.

ACKNOWLEDGEMENT
This work was supported by Natural Science Foundation of Henan Province of China (182300410151), Key Scientific Research Project of College and University in Henan Province (17A610003), Henan Key Laboratory of Industrial Microbial Resources and Fermentation Technology Open Project (HIMFT20200206) and supported by Interdisciplinary Sciences Project, Nanyang Institute of Technology.

References

1. J.L. Andersen, G.-X. He, P. Kakarla, R. KC, S. Kumar, W.S. Lakra, M.M. Mukherjee, I. Ranaweera, U. Shrestha and T. Tran, *International journal of environmental research and public health*, 12 (2015) 1487.
2. Y. Orooji, B. Tanhaei, A. Ayati, S.H. Tabrizi, M. Alizadeh, F.F. Bamoharram, F. Karimi, S. Salmanpour, J. Rouhi and S. Afshar, *Chemosphere*, 281 (2021) 130795.
3. H.A. Almehdar, N. Abd El-Baky, A.A. Alhaider, S.A. Almuhaideb, A.A. Alhaider, R.S. Albiheyri, V.N. Uversky and E.M. Redwan, *Probiotics and antimicrobial proteins*, 12 (2020) 18.
4. H. Karimi-Maleh, Y. Orooji, F. Karimi, M. Alizadeh, M. Baghayeri, J. Rouhi, S. Tajik, H. Beitollahi, S. Agarwal and V.K. Gupta, *Biosensors and Bioelectronics*, 184 (2021) 113252.
5. T. Christidis, M. Hurst, W. Rudnick, K.D. Pintar and F. Pollari, *Food Control*, 109 (2020) 106899.
6. H. Karimi-Maleh, M.L. Yola, N. Atar, Y. Orooji, F. Karimi, P.S. Kumar, J. Rouhi and M. Baghayeri, *Journal of colloid and interface science*, 592 (2021) 174.
7. H. Karimi-Maleh, S. Ranjbari, B. Tanhaei, A. Ayati, Y. Orooji, M. Alizadeh, F. Karimi, S. Salmanpour, J. Rouhi and M. Sillanpää, *Environmental Research*, 195 (2021) 110809.
8. C. Shi, P. Singh, M.L. Ranieri, M. Wiedmann and A.I. Moreno Switt, *Critical reviews in microbiology*, 41 (2015) 309.
9. M. Dar, S. Ahmad, S. Bhat, R. Ahmed, U. Urwat, P. Mumtaz, T. Dar, R. Shah and N. Ganai, *World's Poultry Science Journal*, 73 (2017) 345.
10. Q. Li, W. Cheng, D. Zhang, T. Yu, Y. Yin, H. Ju and S. Ding, *International Journal of Electrochemical Science*, 7 (2012) 844.
11. S. Xu, H. Duo, C. Zheng, S. Zhao, S. Song and G. Simon, *International Journal of Electrochemical Science*, 14 (2019) 1248.
12. P. Skládal, D. Kovář, V. Krajíček, P. Šišková, J. Přibyl and E. Švábenská, *International Journal of Electrochemical Science*, 8 (2013) 1635.

13. B. He and G. Du, *Int. J. Electrochem. Sci*, 11 (2016) 8546.
14. Z. Savari, S. Soltanian, A. Noorbakhsh, A. Salimi, M. Najafi and P. Servati, *Sensors and Actuators B: Chemical*, 176 (2013) 335.
15. M.E. David, R.-M. Ion, R.M. Grigorescu, L. Iancu, E.R. Andrei, R. Somoghi, A.N. Frone and R.M. Stirbescu, *Multidisciplinary Digital Publishing Institute Proceedings*, 57 (2020) 45.
16. Z. Li, J. Yin, C. Gao, L. Sheng and A. Meng, *Microchimica Acta*, 186 (2019) 90.
17. A. Dolati, M. Ghorbani and M. Ahmadi, *Journal of Electroanalytical Chemistry*, 577 (2005) 1.
18. E. Rouya, G.R. Stafford, C. Beauchamp, J. Floro, R. Kelly, M. Reed and G. Zangari, *Electrochemical and Solid State Letters*, 13 (2010) D87.
19. H.M. Alshammari, A.S. Alshammari, J.R. Humaidi, S.A. Alzahrani, M.S. Alhumaimess, O.F. Aldosari and H. Hassan, *Processes*, 8 (2020) 1380.
20. H. Savaloni and R. Savari, *Materials Chemistry and Physics*, 214 (2018) 402.
21. M. Mohammad, A.A. Moosa, J. Potgieter and M.K. Ismael, *International Scholarly Research Notices*, 2013 (2013) 1.
22. H. Yano, K. Kudo, K. Marumo and H. Okuzaki, *Science Advances*, 5 (2019) eaav9492.
23. V. Singh, S. Arora, M. Arora, V. Sharma and R. Tandon, *Semiconductor Science and Technology*, 29 (2014) 045020.
24. J. Rajendran, A.N. Reshetilov and A.K. Sundramoorthy, *Materials Advances*, 2 (2021) 3336.
25. M.N. Norizan, M.H. Moklis, S.Z.N. Demon, N.A. Halim, A. Samsuri, I.S. Mohamad, V.F. Knight and N. Abdullah, *RSC Advances*, 10 (2020) 43704.
26. H. Savaloni, R. Savari and S. Abbasi, *Current Applied Physics*, 18 (2018) 869.
27. R. Savari, H. Savaloni, S. Abbasi and F. Placido, *Sensors and Actuators B: Chemical*, 266 (2018) 620.
28. A.A. Alekseeva, P.M. Rajanna, A.S. Anisimov, O. Sergeev, S. Bereznev and A.G. Nasibulin, *physica status solidi (b)*, 255 (2018) 1700557.
29. S. Huang, M. Lu and L. Wang, *RSC Advances*, 11 (2021) 501.
30. F. Chahshouri, H. Savaloni, E. Khani and R. Savari, *Journal of Micromechanics and Microengineering*, 30 (2020) 075001.
31. H. Savaloni, E. Khani, R. Savari, F. Chahshouri and F. Placido, *Applied Physics A*, 127 (2021) 1.
32. H. Wang, S.-A. He, Z. Cui, C. Xu, J. Zhu, Q. Liu, G. He, W. Luo and R. Zou, *Chemical Engineering Journal*, 420 (2021) 129693.
33. M. Freitas, S. Viswanathan, H.P.A. Nouws, M.B.P.P. Oliveira and C. Delerue-Matos, *Biosensors and Bioelectronics*, 51 (2014) 195.
34. F.-P. Du, N.-N. Cao, Y.-F. Zhang, P. Fu, Y.-G. Wu, Z.-D. Lin, R. Shi, A. Amini and C. Cheng, *Scientific reports*, 8 (2018) 1.
35. L. Sha, P. Gao, T. Wu and Y. Chen, *ACS applied materials & interfaces*, 9 (2017) 40412.
36. I. Deretzis and A. La Magna, *Nanotechnology*, 17 (2006) 5063.
37. R.Y. Lai, E.T. Lagally, S.-H. Lee, H.T. Soh, K.W. Plaxco and A.J. Heeger, *Proceedings of the National Academy of Sciences of the United States of America*, 103 (2006) 4017.
38. R. Luo, Y. Li, X. Lin, F. Dong, W. Zhang, L. Yan, W. Cheng, H. Ju and S. Ding, *Sensors and Actuators B: Chemical*, 198 (2014) 87.
39. B.S. Ferguson, S.F. Buchsbaum, J.S. Swensen, K. Hsieh, X. Lou and H.T. Soh, *Analytical Chemistry*, 81 (2009) 6503.
40. D. Berdat, A.C.M. Rodríguez, F. Herrera and M.A. Gijs, *Lab on a Chip*, 8 (2008) 302.
41. M. Díaz-Serrano, A. Rosado, D. Santana, E.Z. Vega and A.R. Guadalupe, *Journal of Physics: Conference Series*, 421 (2013) 012008.
42. Q. Li, W. Cheng, D. Zhang, T. Yu, Y. Yin, H. Ju and S. Ding, *Int. J. Electrochem. Sci*, 7 (2012) 844.
43. K. Ikebukuro, Y. Kohiki and K. Sode, *Biosensors and Bioelectronics*, 17 (2002) 1075.

44. D. Zhang, Y. Yan, Q. Li, T. Yu, W. Cheng, L. Wang, H. Ju and S. Ding, *Journal of Biotechnology*, 160 (2012) 123.
45. B. Priyanka, R.K. Patil and S. Dwarakanath, *The Indian journal of medical research*, 144 (2016) 327.
46. N. Paniel and T. Noguer, *Foods*, 8 (2019) 371.